ELECTRONIC SUPPLEMENTARY INFORMATION

Electronic and optical properties of nanostructured MoS_2 materials: Influence of reduced spatial dimensions and edge effects

Vladan Mlinar*

S1 Technical details on our tight-binding (TB) calculations

Tight-binding (TB) model, as implemented in this work includes non-orthogonal sp^3d^5 orbitals and spin-orbit coupling.[1–4]

We are solving a generalized eigenvalue problem:

$$\sum_{b',\beta} H^{b,b'}_{\alpha,\beta}(\mathbf{k}) C_{\mathbf{k},n}(b',\beta) = \varepsilon_n(\mathbf{k}) \sum_{b',\beta} S^{b,b'}_{\alpha,\beta}(\mathbf{k}) C_{\mathbf{k},n}(b',\beta) \ , \tag{S1}$$

where H and S are TB Hamiltonian and overlap matrix, respectively. $\varepsilon_n(\mathbf{k})$ are eigenvalues and $C_{\mathbf{k},n}$ the expansion coefficients for the eigenvectors of the band n. b (b') labels a basis atom, and α (β) orbital types on that atom.

As already mentioned in the main body of the manuscript, the description of Hamiltonian H and the overlap matrix S for MoS_2 is attained by employing a set of 96 TB parameters that describe the on-site orbital energies, the Slater-Koster energy integrals, overlap integrals, and the spin-orbit interaction, as given in Refs.[5,6] For intra-layer S-S, Mo-S, and Mo-Mo interactions we consider nearest-neighbor and for inter-layer S-S interactions the second nearest neighbor hopping and overlap matrix elements. TB parameter-sets are listed in Sec. S2.

The spin-orbit interaction is assumed to couple only intra-atomic states with nonzero angular momentum,[7–9] i.e., $\lambda_a \hat{\mathbf{L}}_a \cdot \hat{\mathbf{S}}_a$, where $a = Mo, S$, λ is the intra-atomic spin-orbit parameter. * $\hat{\mathbf{L}}$ and $\hat{\mathbf{S}}$ are the angular momentum operator and spin operator, respectively.

The size of our TB and overlap matrices is $N_{TB} \times N_{TB}$, where $N_{TB} = (N_S N_{S_{orbitals}} + N_{Mo} N_{Mo_{orbitals}}) \times 2$. N_S (N_{Mo}) is number of S (Mo) atoms, and $N_{S_{orbitals}}$ ($N_{Mo_{orbitals}}$) is the number of S (Mo)-orbitals included in TB model, in our case $N_{S_{orbitals}} = N_{Mo_{orbitals}} = 9$. Factor 2 is due to spin. Given that we include only nearest-neighbor interaction (and second-nearest for S-S for interlayer interaction), our matrices are sparse. Thus, as it is a standard practice, only non-zero matrix elements are stored to memory.

In general, if properly parametrized, TB is considered to be an accurate atomistic representation of nanostructured materials containing $> 10^3$ (even up to a few million) atoms; results on electronic, optical, and transport properties of TB method have typically shown a good agreement with experiment and impressive predictive potential.[3,4,9–11]

Density of States (DOS) is defined as:

$$D(E) = \sum_{\mathbf{k},n} \delta(E - \varepsilon_{\mathbf{k},n}) \ , \tag{S2}$$

Research Institute for Advanced Materials Design, Providence, RI 02906, USA. E-mail: vladan.mlinar@riamd.org; Tel: (+1)401-573-9191

* In our implementation we can treat different values of λ for p- and d-orbitals.

Partial DOS of an orbital α in the atom b is given by:

$$D_{b\alpha}(E) = \sum_{\mathbf{k},n} \delta(E - \varepsilon_{\mathbf{k},n}) C^{\dagger}_{\mathbf{k},n}(b,\alpha) S(\mathbf{k}) C_{\mathbf{k},n}(b,\alpha) \ . \tag{S3}$$

We remind the reader that for any two band indexes n and m: $C^{\dagger}_{\mathbf{k},n} S(\mathbf{k}) C_{\mathbf{k},m} = \delta_{nm}$.

In solving Eqs. (S2) and (S3) we use Lorentzian-broadening function instead of Dirac delta function, $\delta(E - \varepsilon_{\mathbf{k},n}) \to \Gamma/(\pi(\Gamma^2 + (E - \varepsilon_{\mathbf{k},n})^2))$. Typically broadening of $\Gamma = 30$ meV is assumed in our calculations.

The real part of optical conductivity in the dipole approximation can be obtained from: [12–18]

$$Re[\sigma(\omega)] = \frac{\pi e^2}{2\hbar\omega m_e^2} \sum_{n}^{occ} \sum_{m}^{empty} \int_{1BZ} \frac{d^3\mathbf{k}}{(2\pi)^2} |p_{nm}(\mathbf{k})|^2 \delta(\varepsilon_{m,\mathbf{k}} - \varepsilon_{n,\mathbf{k}} - \hbar\omega) \ , \tag{S4}$$

where $\hbar\omega$ is the photon energy, p_{nm} is the momentum matrix element, and ε_n and ε_m are energies of nth and mth bands, respectively. Also, e denotes the electron charge and m_e the electron mass. The integration is carried over the first Brillouin zone (1BZ). For more details regarding Eq. (S4) see e.g., Refs. [13,14].

The momentum matrix element, p_{nm}, is defined as:

$$p_{nm}(\mathbf{k}) = \langle \Psi_m(\mathbf{k}) | \, \hat{\mathbf{e}}\mathbf{p} \, | \Psi_n(\mathbf{k}) \rangle \ , \tag{S5}$$

where $\hat{\mathbf{e}}$ is direction of polarization of the incident light and $\mathbf{p}$ is the momentum operator.

We calculate $p_{nm}(\mathbf{k})$, Eq. (S5), directly from the TB Hamiltonian and the expansion coefficients for the eigenvectors, [15,16] without the need for additional parameters. Namely, [15]

$$p_{nm}(\mathbf{k}) = \sum_{b\alpha,b'\alpha'} = C^{\dagger}_{\mathbf{k},n}(b,\alpha) C_{\mathbf{k},m}(b',\alpha') \sum_{\mathbf{R}} e^{i\mathbf{k}\mathbf{R}} \mathbf{R} E^{bb'}_{\alpha\alpha'}(\mathbf{R}) \ , \tag{S6}$$

where $E^{bb'}_{\alpha\alpha'}(\mathbf{R})$ is the Slater-Koster matrix of tight-binding parameters, [1] defined using our input TB parameter set. [5,6]

In solving Eq. (S4) instead of Dirac delta function we employ Lorentzian-broadening function.

For completeness, for calculating the real part of optical conductivity in Eq. (S4) we consider only interband transitions. There is, however an additional contribution to the optical conductivity, coming from intraband transitions. Because momentum conservation is not satisfied for direct absorption of a photon by an intraband optical transition, [14] these transitions depend on lattice imperfections (and temperature). Intraband (Drude) contributions can be estimated from: [19–21]

$$Re[\sigma^{intra}(\omega)] = \frac{\pi e^2}{2\hbar\omega m_e^2} \delta(\hbar\omega) \sum_{n} \int_{1BZ} \frac{d^3\mathbf{k}}{(2\pi)^2} |p_{nn}(\mathbf{k})|^2 \delta(E_F - \varepsilon_{n,\mathbf{k}}) \ . \tag{S7}$$

where $Re[\sigma^{intra}(\omega)]$ can be calculated exploiting the following identity: $p^{\alpha}_{nn} = 2\partial\varepsilon_{n,\mathbf{k}}/\partial k_{\alpha}$, where $\alpha = x, y, z$, see e.g., Ref. [19]

Given that Drude contribution depends on lattice imperfections, it is often represented using phenomenological expression: [14,22] $Re[\sigma^{intra}(\omega)] = \sigma_0/(1 + \omega^2\tau_D^2)$, where σ_0 and τ_D denote dc conductivity and the electron scattering time, respectively. There has been intensive discussion in literature whether this contribution is sufficient, given that it only contributes to the isotropic part of the optical conductivity tensor, [20,23] or it is necessary to include off-diagonal terms. [21] In general, it was agreed this contribution can be neglected

for energies higher than $\sim$1 eV.[14,20,21] In this work, the contribution of intraband transitions to the real part of optical conductivity was neglected.

Next, the total electron density (TED) and partial electron density (PED) are evaluated from:

$$\rho(\mathbf{r}) = \sum_i n_i |\Psi_i(\mathbf{r})|^2 \,, \tag{S8}$$

where n_i is the occupation of state Ψ_i.

Inspired by the number of numerical reports on PED of MoS_2 nanoparticles, experimentally obtained STM images, and linking PED with STM images on isolated MoS_2 nanostructures,[24–27] we calculate TED and PED for our isolated model MoS_2 nanodisks; consequently, $\mathbf{k} = 0$ in our calculations.

Using the expansions coefficients $C_{\mathbf{k}=\mathbf{0},i}(b,\alpha) = C_i(b,\alpha)$, which are the output of TB calculations and contain information about basis atoms and corresponding orbitals [see also Eq. (S1)], we construct $\Psi_i(\mathbf{r})$ by:

$$\Psi_i(\mathbf{r}) = \sum_{b,\alpha} C_i(b,\alpha) r_{b,nl}(\mathbf{r}-\mathbf{R_b}) Y_{lm}(\mathbf{r}-\mathbf{R_b}) \,, \tag{S9}$$

where $r_{b,nl}(\mathbf{r}-\mathbf{R_b})Y_{lm}(\mathbf{r}-\mathbf{R_b})$ represent atomic basis orbitals for a basis atom b located at $\mathbf{R_b}$. It includes the radial part, which is numerically adjusted (see below) and spherical harmonic $Y_{lm}(\mathbf{r}-\mathbf{R_b})$. n, l, and m denote principal, angular, and magnetic quantum numbers, respectively.

The radial part $r_{b,nl}$ is tuned taking into account d-d orbital interactions for Mo-Mo, p-d orbital interactions for S-Mo, and p-p for S-S. We allow for radial functions of Mo and S to have different cut-off radia. Results for the calculated TED and PED for our MoS_2 nanodisk is shown in Figure 8 in the main body of the manuscript.

S2 Tight-binding parameter sets

We use a set of ninety six parameters proposed and derived in Refs.[5,6], which were fitted to the band structure of monolayer (1ML), bilayer (2ML), and bulk MoS_2 obtained from DFT with HSE06 functional.[5,6] The parameters are listed in Table S1. This TB parameter set is also denoted as *TB set 1* in Sec. 3.2 in the main body of the manuscript where we compare the lowest conduction band and the highest valence band for 1ML MoS_2 calculated using three different parameter sets.

As discussed in the main body of the manuscript [Sec. 3.2], alternative MoS_2 TB parameter sets were proposed to describe the band structure of 1ML of MoS_2. A TB model based on those parameter sets assumes eleven orthogonal orbitals (4*d* Mo and 3*p* S) to describe CBM and VBM of 1ML MoS_2, requiring 12 (+2 for spin-orbit coupling) parameters. Cappelluti *et al.* in Refs.[8,29] derived TB parameters which we refer to as *TB set 2* in Sec. 3.2, and Ridolfi *et al.* in Ref.[30] parameters referred to as *TB set 3*. We remind the reader that detailed comparison between TB calculations using *TB set 1*, *TB set 2*, and *TB set 3* is given in Sec. 3.2.

Table S2 contains parameters of *TB set 2* and Table S3 parameters of *TB set 3*. We note Cappelluti *et al.*, *TB set 2*, also proposed two additional parameters to model the lowest conduction band and the highest valence band of bulk MoS_2; a reasonable agreement with DFT calculations was found around *K* point.[8,29]

Table S1 Tight-binding parameter set for MoS_2 as proposed in Refs.[5,6] and used in this work. Intra-atomic spin-orbit parameters are taken from Ref.[28]. Also, this parameter set is referred to as *TB set 1* in Sec. 3.2.

On-site energies (in eV)			Spin-orbit parameter (in eV)		
	S	Mo		S	Mo
E_s	8.21704600	5.56599100	λ	0.05700000	0.13000000
E_p	-2.00758000	7.47501400			
E_d	9.05457100	2.00856100			

Slater-Koster energy integrals (in eV)					
	intra-layer				inter-layer
	S-S	S-Mo	Mo-S	Mo-Mo	S-S
$V_{ss\sigma}$	0.35039000	-0.40357580	-0.40357580	0.20175660	0.09593108
$V_{sp\sigma}$	-0.88529290	0.47482550	1.40922000	1.09058100	0.29708310
$V_{sd\sigma}$	-0.25082810	0.59497540	-0.57651860	-0.41934230	0.13338260
$V_{pp\sigma}$	0.75877300	1.50083700	1.50083700	-0.77366480	0.78874210
$V_{pp\pi}$	-0.17854660	-0.44403510	-0.44403510	0.55548210	-0.09046535
$V_{pd\sigma}$	-0.48367680	-2.92015000	-2.12676700	-0.27166720	-0.15754920
$V_{pd\pi}$	-0.05438542	0.87967080	2.07882900	0.13757700	0.00692037
$V_{dd\sigma}$	0.69155650	-3.24960500	-3.24960500	0.08963398	-0.08309669
$V_{dd\pi}$	0.92089080	2.36485200	2.36485200	0.12100610	0.28221060
$V_{dd\delta}$	-0.12831850	-0.38452100	-0.38452100	0.09734699	-0.00555235

Overlap integrals					
	intra-layer				inter-layer
	S-S	S-Mo	Mo-S	Mo-Mo	S-S
$O_{ss\sigma}$	-0.08986125	0.05725651	0.05725651	-0.07436093	-0.02666435
$O_{sp\sigma}$	-0.02968737	-0.02521967	-0.11652550	-0.04082800	-0.04285134
$O_{sd\sigma}$	0.06398180	0.02522340	-0.12473430	-0.13278140	-0.00695736
$O_{pp\sigma}$	0.03247643	-0.11079410	-0.11079410	0.02904314	-0.07211146
$O_{pp\pi}$	-0.02765439	0.04323795	0.04323795	0.03756407	-0.00804274
$O_{pd\sigma}$	0.09256573	0.10676990	-0.21366630	-0.01685267	0.00714757
$O_{pd\pi}$	0.07367491	-0.00825893	0.20296200	-0.03728849	0.03526020
$O_{dd\sigma}$	0.31860380	-0.00700407	-0.00700407	-0.04149141	-0.06104299
$O_{dd\pi}$	0.06890423	0.15131840	0.15131840	-0.01814713	-0.03877815
$O_{dd\delta}$	0.02819366	0.15207940	0.15207940	0.00874711	-0.02324867

S3 Applicability of our TB approach from bulk, surfaces, to nanostructures: Issue of local charge neutrality

The issue: One of the major challenges in the application of a parametrized (semi-empirical) TB model for the electronic structure calculation of nanostructured materials is the development of transferable parameters that can be reliably used for bulk, surfaces, nanowires and nanodisks. The problem is to account for interatomic charge redistribution in surfaces, heterojunctions, or geometrically inhomogeneous systems in general.[3,31,32] If not properly treated, which is the case for a standard TB parametrization, nonphysically large charge transfers occur leading to displacements of surface states and the distortion of DOS.[31,32]

Background and proposed solutions: The TB on-site matrix elements are a function of the local environment around each atom. In TB parametrization, on-site energies either use *ad hoc* models for the variation of TB on-site elements with changes in the environment, or the on-site energies are fixed and typically fitted to reproduce the bulk band structure.[3] In the former, the arbitrariness leads to a lack of physical transparency in TB models and increases the number of independent parameters that need to be used, whereas in the latter case this could lead to problems in calculating the charges for nanostructured systems or systems with non-equivalent basis atoms. In order to avoid nonphysical results due to large charge transfers, imposing a

Table S2 Tight-binding parameter set for 1ML MoS_2 as proposed in Refs.[8,29], referred to as *TB set 2* in Sec. 3.2. Cappelluti *et al.* also proposed two additional parameters to model the lowest conduction band and the highest valence band of bulk MoS_2 (see text).

On-site energies (in eV)		
	S	Mo
$E_{p_x} = E_{p_y}$	-1.276	0.000
E_{p_z}	-8.236	0.000
$E_{d_{xy}} = E_{d_{x^2-y^2}}$	0.000	-3.025
$E_{d_{xz}} = E_{d_{yz}}$	0.000	0.419
$E_{d_{3z^2-r^2}}$	0.000	-1.512

Spin-orbit parameter (in eV)		
	S	Mo
λ	0.052	0.075

Slater-Koster energy integrals (in eV)					
	intra-layer				inter-layer
	S-S	S-Mo	Mo-S	Mo-Mo	S-S
$V_{pp\sigma}$	0.696	0.000	0.000	0.000	-0.774
$V_{pp\pi}$	0.278	0.000	0.000	0.000	0.123
$V_{pd\sigma}$	0.000	-2.619	-2.619	0.000	-
$V_{pd\pi}$	0.000	-1.396	-1.396	0.000	-
$V_{dd\sigma}$	0.000	0.000	0.000	-0.933	-
$V_{dd\pi}$	0.000	0.000	0.000	0.478	-
$V_{dd\delta}$	0.000	0.000	0.000	-0.442	-

constraint for the charge becomes necessary.[3,32]

This problem originates from the non-self-consistent nature of the potential. In *ab initio* calculations, the Hamiltonian is solved self-consistently and a quasi-charge neutrality of each atom is found.[31] In a parametrized TB model the charge density is not known and the self-consistency problem cannot be solved without introducing new parameters describing Coulomb interactions between electrons.[3]

Keeping in mind that TB model should be, from one side as simple as possible to be used to calculate the electronic, optical, and transport properties of complex nanostructured materials, and from the other, to capture all the relevant microscopic features of materials, two paths for fixing local charge neutrality issue were proposed: (i) to introduce self-consistency in order to correctly represent charge transfer effects in non-bulk-like bonding environments; the on-site energies are shifted until the system reaches a stable equilibrium with respect to the charges, the local charge neutrality constraint. (ii) local environment dependent on-site energy levels are introduced into the TB parametrization, typically orthogonal TB parameters-scheme, but also including intra-atomic interactions.[3]

One problem with introducing self-consistency are additional parameters, as well as increased computational time. That is why option (ii) sounded appealing; it was shown that this maximized the flexibility of the scheme for a wide range of applications, e.g., it gives a good description of electronic properties of nanostructured metal-based systems.[3,33] Of course, further improvement would use self-consistent charge density-functional based TB method, see, e.g., Refs.[34,35].

Our approach: TB parameter set used in this work (Refs.[5,6]) provide good description of the band structure of 1ML, 2ML, and bulk MoS_2 (see Sec. 3, including Fig. 2, Table 1 and Table 2, in the main body of the manuscript). Thus, the case where surface atoms (S-atoms) in 1ML of MoS_2 have different local environment compared to the bulk case is included in the TB parametrization.[6]

Furthermore, for nanostructured MoS_2 materials, our results show good agreement with the findings extracted from DFT-based calculations. Specifically, our results on DOS of nanodisks agree with those extracted from DFT calculations in Ref.[27], discussed throughout Sec. 4 in the main body of the manuscript. Also, we run test case for the band structure of nanoribbons as defined in Ref.[36], and found good agree-

Table S3 Tight-binding parameter set for 1ML MoS_2 as proposed in Ref.[30], referred to as *TB set 3* in Sec. 3.2.

On-site energies (in eV)			Spin-orbit parameter (in eV)		
	S	Mo		S	Mo
$E_{p_x} = E_{p_y}$	-54.839	0.000	λ	0.00052	0.075
E_{p_z}	-39.275	0.000			
$E_{d_{xy}} = E_{d_{x^2-y^2}}$	0.000	-0.352			
$E_{d_{xz}} = E_{d_{yz}}$	0.000	-1.563			
$E_{d_{3z^2-r^2}}$	0.000	0.201			

Slater-Koster energy integrals (in eV)					
	intra-layer				inter-layer
	S-S	S-Mo	Mo-S	Mo-Mo	S-S
$V_{pp\sigma}$	12.734	0.000	0.000	0.000	-
$V_{pp\pi}$	-2.175	0.000	0.000	0.000	-
$V_{pd\sigma}$	0.000	-9.880	-9.880	0.000	-
$V_{pd\pi}$	0.000	4.196	4.196	0.000	-
$V_{dd\sigma}$	0.000	0.000	0.000	-1.153	-
$V_{dd\pi}$	0.000	0.000	0.000	0.612	-
$V_{dd\delta}$	0.000	0.000	0.000	0.086	-

ment. Finally, we have not found *any* non-physical solutions. We remind the reader that in this work we are focused on identifying universal features in the electronic structure, and not on influence of specific structural features because they either could not be detected in structural characterization or they cannot be captured by our present model (see additional discussion in Sec. S1 and S4). We stress here, as we do in the main body of the manuscript, for detailed modeling of edge effects, one would need to use more complex models, e.g. within TB approximation, self-consistent charge density-functional based TB method.

As a side note, when comparing our results with those extracted using TB parameter sets *TB set 2* and *TB set 3* [Sec.3.2 and Fig. 3 in the main body of the manuscript], we see that those parameter sets are not transferable; they are limited only to 1ML. For example, the proposed additional two parameters in *TB set 2* [see also Sec. S2] for the description of the band structure of bulk MoS_2, provided a reasonable description of the band structure only around K point.

S4 Model structures of nanostructured MoS_2 materials: Structure from experiment versus theory

In our model structures we use optimized unreconstructed edges. Our model structures are constructed taking into account experimental findings (see below) and other theoretical models (for nanoribbons in Ref.[36] and nanodisks in Ref.[27]).

Regarding model structures versus structural characterization, we note that in the experimental situations additional factors often come into play, such as for example substrate effects, possible existence of additional sulfur and/or hydrogen,[36,37] etc. Whereas STM images were matched to numerical calculations,[26,27] challenges in characterizing the edge structures experimentally, prevent us from determining how MoS_2 edges reconstruct. For additional discussion see e.g., Refs.[36,37]

Nanowires: the width d_{wire} is calculated using formula: $d_{wire} \approx (a/\sqrt{3})n_{hex}$, where n_{hex} represents approximate number of hexagon side lengths included in the width of the nanowire.

Nanodisks: Nanodisks are characterized by the number of Mo and S atoms, as well as the number (N) of Mo atoms on the edge of nanodisks, which gives edge length $d = (N-1)a_{latt}$, $a_{latt} = 3.179\mathring{A}$.

Specifically,
For nanodisks in Fig. 7(a) top panel:
disk 1: $Mo_{132}S_{312}$ and N = 11
disk 2: $Mo_{121}S_{334}$ and N = 11
disk 3: $Mo_{96}S_{254}$ and N = 11

For nanodisks in Fig. 7(a) bottom panel:
disk 1 ($d_1 = d_2$): $Mo_{36}S_{112}$ and N = 6
disk 1 ($d_1 < d_2$): $Mo_{186}S_{512}$ and $N_1 = 6$, $N_2 = 31$
disk 1 ($d_1 > d_2$): $Mo_{126}S_{322}$ and $N_1 = 21$, $N_2 = 6$

For nanodisk in Figs. 8 and 9:
disk 1: $Mo_{36}S_{112}$ and N = 6

S5 Additional results on electronic properties of MoS_2 nanostructured materials

In the main body of the manuscript we discussed how electronic and optical properties of nanostructured MoS_2 materials are influenced by reducing spatial dimensions and edge effects. In this Section of Electronic Supplementary Information we provide additional results on DOS of MoS_2-based nanowires and disks.

Electronic properties of MoS_2 nanowires

Figure S1 shows how calculated DOS of nanowires is affected by edge effects depending on the size (d_{wire}) of the wire.

For a nanowire with d_{wire} = 2.9 nm the difference in edge atoms [see Fig. 4(a)] is reflected in DOS. However, as intuitively expected, with increasing size of the wire the influence of the edge of DOS is reduced. It turns out that for a nanowire size d_{wire} = 9.2 nm, role of edge "decoration" on DOS becomes negligible.

As a test of our calculations, Figure S2 demonstrates how calculated DOS changes with increasing d_{wire} and for d_{wire} = 31.5 nm resembles DOS of MoS_2 1ML sheet.

Electronic properties of MoS_2 nanodisks

As it was discussed in Ref.[26] and in the main body of the manuscript, resolving edge states is very tricky and requires combination of input from DFT as well as experimentally obtained STM images. Further complication could be introduced by potential surface defects, i.e., S atoms missing.

Figure S3 shows calculated DOS of the *disk1* with d = 1.59 nm (N = 6) as it changes in the presence of surface defects; defect I is 2S atoms missing from the right edge and defect II – 2S atoms missing from the top right corner of the disk. Fig. S3(b) shows zoomed in DOS around Fermi energy.

We see that here considered surface defects introduce variations in E_F less than 30 meV for *disk1* $Mo_{36}S_{96}$ vs $Mo_{36}S_{94}$. The changes however do not influence "visibility" of disks in a STM image; as seen in Fig. S3(b), E_F for different surface defects still reside near a local maximum in DOS. Given that here we are focused on "more universal" robust effects that are not limited to special cases, we consider scenarios where one or two whole edges of nanodisk lacking S atoms.

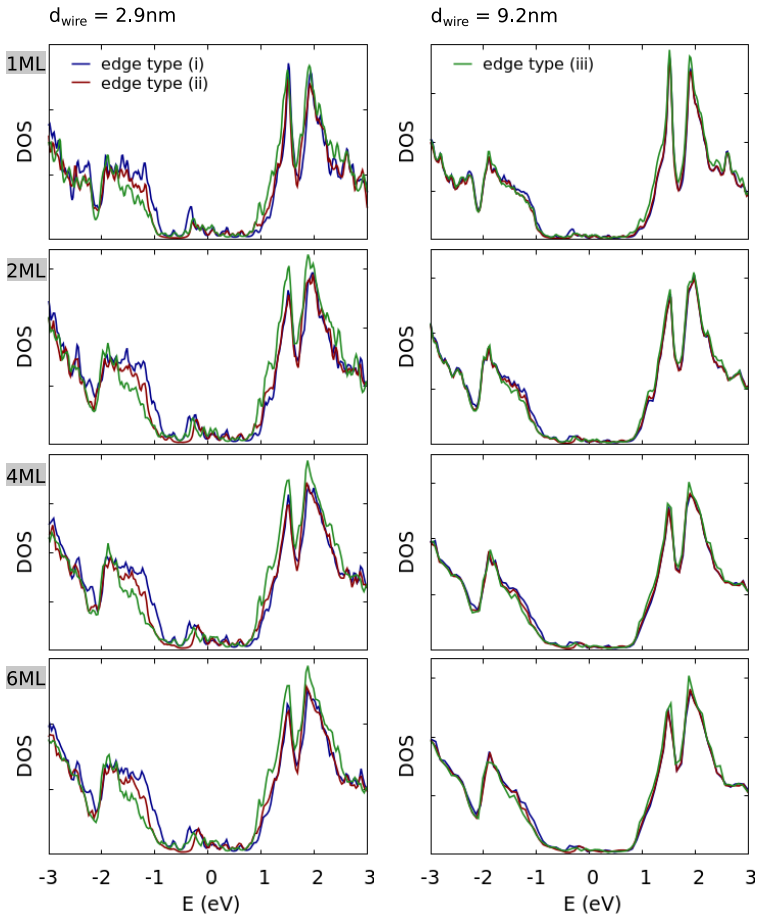

Fig. S1 Calculated density of states (DOS) for nanowires of size d_{wire} = 2.9 nm and d_{wire} = 9.2 nm with different number of monolayers and different edge-types [type i, type ii, and type iii, as shown in Fig. 4(a)].

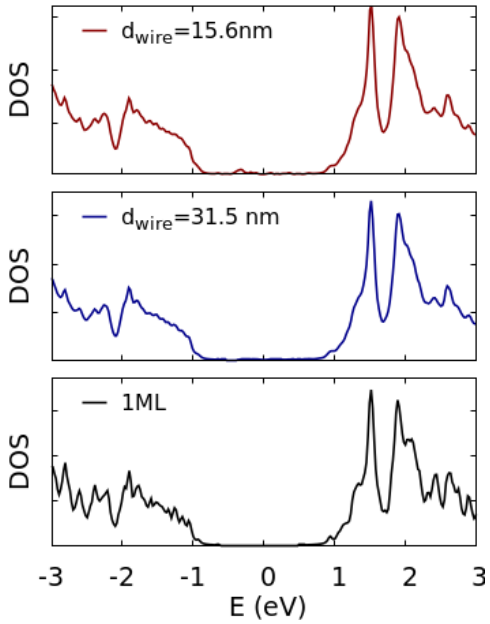

Fig. S2 Calculated DOS for nanowires of size d_{wire} = 15.6 nm and d_{wire} = 31.5 nm as they compare with calculated DOS for 1ML sheet MoS_2.

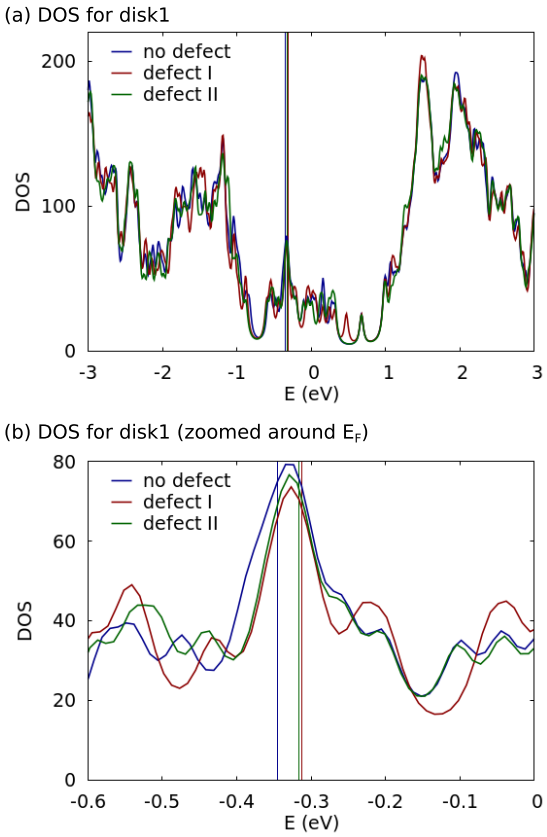

Fig. S3 (a) Calculated DOS of the *disk1* with d = 1.59 nm as it changes in the presence of surface defects; defect I is 2S atoms missing from the right edge and defect II – 2S atoms missing from the top right corner of the disk; (b) shows zoomed in DOS around Fermi energy.

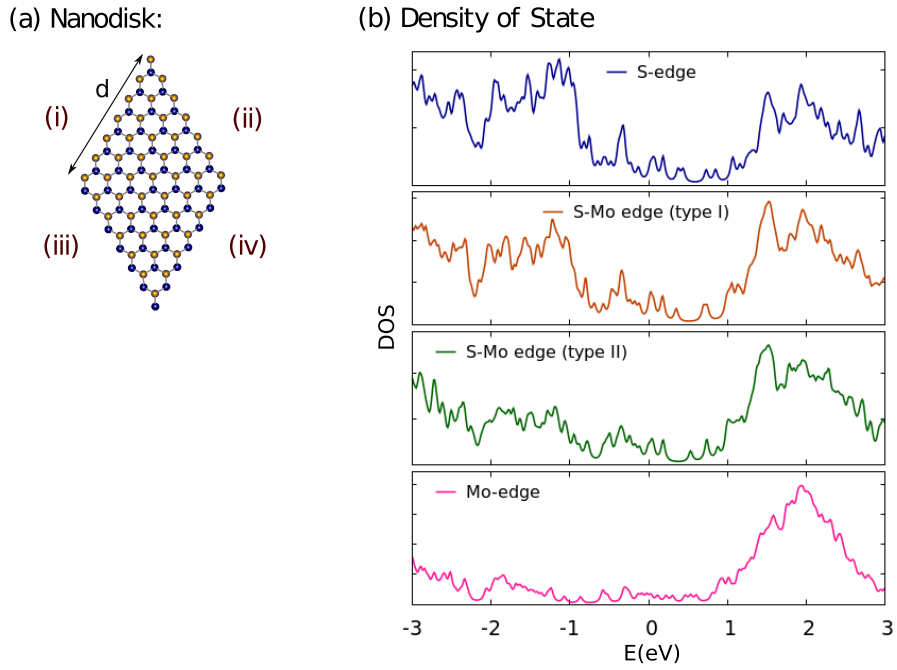

Fig. S4 (a) nano-disk with d = 1.59 nm; (i)-(iv) denote edges of the disk. (b) Calculated DOS for nano-disk as we vary S coverage on edges; from top to bottom: *S-edge* – 100% S coverage on all four edges; *S-Mo (type I)* – 100% S coverage on edges (i), (iii), and (iv), and S-atoms removed from the edge (ii); *S-Mo (type II)* – 100% S coverage on the edges (iii) and (iv), S-atoms removed from the edges (i) and (ii); and *Mo-edge* – S-atoms removed from all four edges.

Figure S4 shows calculated DOS of a nanodisk with d = 1.59 nm [see also Fig. 1(c) in the main body of the manuscript] as it varies with atom-types on edges [(i)-(iv)] of the disk. Following edge-types are analyzed: *S-edge* – 100% S coverage on all four edges; *S-Mo (type I)* – 100% S coverage on edges (i), (iii), and (iv), and S-atoms removed from the edge (ii); *S-Mo (type II)* – 100% S coverage on the edges (iii) and (iv), S-atoms removed from the edges (i) and (ii); and *Mo-edge* – S-atoms removed from all four edges.

As discussed in the manuscript, valence states originate from p-orbitals of S-atoms, mainly at the interface, and conduction states from d-orbitals of Mo atoms. With changing a "decoration" at the edges of the disk, we are influence density of states in valence and conduction band. Given that valence band is mainly determined by the S atoms at the interface, we see that in the hypothetical case of Mo-edge, valence band states are almost completely suppressed.

Next, in Fig. S4(b), DOS for S-edge and S-Mo edge (type I) exhibit peak caused by Mo atoms terminated by S dimers on the edge, see also the discussion in the main body of the manuscript. For nano-disks with S-Mo edge (type II) this peak reduces and finally disappears for Mo-edge case.

References

1 J. C. Slater and G. F. Koster, *Phys. Rev.*, 1954, **94**, 1498–1524.
2 D. A. Papaconstantopoulos and M. J. Mehl, *J. Phys.: Condens. Matter*, 2003, **15**, R413–R440.
3 G. Hegde, M. Povolotskyi, T. Kubis, T. Boykin and G. Klimeck, *J. Appl. Phys.*, 2014, **115**, 123703.
4 V. Mlinar, *J. Mater. Chem.*, 2012, **22**, 1724–1732.
5 F. Zahid, *Private communication*.
6 F. Zahid, L. Liu, Y. Zhu, J. Wang and H. Guo, *AIP Adv.*, 2013, **3**, 052111.
7 D. J. Chadi, *Phys. Rev. B*, 1977, **16**, 790.
8 R. Roldán, M. P. López-Sancho, F. Guinea, E. Cappelluti, J. A. Silva-Guillén and P. Ordejón, *2D Materials*, 2014, **1**, 034003:1–034003:21.

9 S. Yuan, R. Roldán, M. I. Katsnelson and F. Guinea, *Phys. Rev. B*, 2014, **90**, 041402(R):1 – 041402(R):4.
10 M. Luisier, A. Schenk, W. Fichtner and G. Klimeck, *Phys. Rev. B*, 2006, **74**, 205323:1–205323:12.
11 G. W. Bryant, M. Zieliński, N. Malkova, J. Sims, W. Jaskólski and J. Aizpurua, *Phys. Rev. Lett.*, 2010, **105**, 067404.
12 C. S. Wang and J. Callaway, *Phys. Rev. B*, 1974, **90**, 4897–4907.
13 M. Gibertini, F. M. D. Pellegrino, N. Marzari and M. Polini, *Phys. Rev. B*, 2014, **90**, 245411:1–245411:8.
14 H. Ebert, *Rep. Prog. Phys.*, 1996, **59**, 1665–1735.
15 L. C. L. Y. Voon and L. R. Ram-Mohan, *Phys. Rev. B*, 1993, **47**, 15500–15508.
16 B. Jogai, *Solid State Commun.*, 2000, **116**, 153–157.
17 D. L. Dexter, *Solid State Phys.*, 1958, **6**, 353–411.
18 F. Trani, G. Cantele, D. Ninno and G. Iadonisi, *Phys. Rev. B*, 2005, **72**, 075423:1–075423:8.
19 I. V. Solovyev, *Phys. Met. Metallogr.*, 2001, **91**, S199.
20 E. G. Maksimov, I. I. Mazin, S. N. Rashkeev and Y. A. Uspenski, *Journal of Physics F: Metal Physics*, 1988, **18**, 833.
21 J. L. Erskine and E. A. Stern, *Phys. Rev. B*, 1973, **8**, 1239–1255.
22 K. F. Mak, L. Ju, F. Wang and T. F. Heinz, *Solid State Commun.*, 2012, **152**, 1341–1349.
23 I. I. Mazin, E. M. Savitskii and Y. A. Uspenskii, *Journal of Physics F: Metal Physics*, 1984, **14**, 167.
24 J. Tersoff and D. R. Hamann, *Phys. Rev. B*, 1985, **31**, 805–813.
25 T. F. Fässler, U. Häussermann and R. Nesper, *Chem. Eur. J.*, 1995, **1**, 625–633.
26 Lauritsen Jeppe V., Kibsgaard Jakob, Helveg Stig, Topsoe Henrik, Clausen Bjerne S., Laegsgaard Erik and Besenbacher Flemming, *Nat Nano*, 2007, **2**, 53–58.
27 T. Li and G. Galli, *J. Chem. Phys. C*, 2007, **111**, 16192–16196.
28 S. Salehi and A. Saffarzadeh, *Surface Science*, 2016, **651**, 215–221.
29 E. Cappelluti, R. Roldaán, J. A. Silva-Guillén, P. Ordejón and F. Guinea, *Phys. Rev. B*, 2013, **88**, 075409.
30 E. Ridolfi, D. Le, T. S. Rahman, E. R. Mucciolo and C. H. Lewenkopf, *J. Phys.: Condens. Matter*, 2015, **27**, 365501:1–365501:21.
31 C. Barreteau, D. Spanjaard and M. C. Desjonquères, *Phys. Rev. B*, 1998, **58**, 9721–9731.
32 Y. Xie and J. A. Blackman, *Phys. Rev. B*, 2001, **64**, 195115.
33 G. Hegde, M. Povolotskyi, T. Kubis, J. Charles and G. Klimeck, *J. Appl. Phys.*, 2014, **115**, 123704.
34 J. Wang, X. Dai, W. Jiang, T. Yu and Z. Wang, *International Journal of Quantum Chemistry*, 2017, **117**, e25320–n/a.
35 M. Elstner, T. Frauenheim, E. Kaxiras, G. Seifert and S. Suhai, *Phys. Stat. Sol. (b)*, 2000, **217**, 357–376.
36 P. Cui, J.-H. Choi, W. Chen, J. Zeng, C.-K. Shih, Z. Li and Z. Zhang, *Nano Letters*, 2017, **17**, 1097–1101.
37 J. Gao, X. Liu, G. Zhang and Y.-W. Zhang, *Nanoscale*, 2016, **8**, 17940–17946.